

GALACTIC KINEMATICS OF PLANETARY NEBULAE WITH [WC] CENTRAL STAR¹

Miriam Peña,² Jackeline S. Rechy-García,² and Jorge García-Rojas^{3,4}

Received 2012 October 18; accepted 2013 January 16

RESUMEN

Usando espectros de alta resolución, analizamos la distribución y cinemática galáctica de nebulosas planetarias con estrella central [WR] y ‘wels’ ([WR]PN y WLPN). Se calcularon las velocidades circulares y peculiares (V_{pec}) de los objetos, y obtuvimos que: (a) Las [WR]PNe pertenecen al disco galáctico y están más concentradas que las WLPNe y PN normales, lo que corresponde a objetos más jóvenes. (b) Clasificamos la muestra en Tipos de Peimbert y encontramos que las PNe de Tipo I tienen $V_{\text{pec}} \leq 50 \text{ km s}^{-1}$, como corresponde a objetos jóvenes; la mayoría de las [WR]PN son del Tipo II con $V_{\text{pec}} \leq 60 \text{ km s}^{-1}$, aunque un porcentaje de la muestra es del Tipo III con V_{pec} más alta, lo que indica que el fenómeno Wolf-Rayet en estrellas centrales puede ocurrir con cualquier masa estelar y en objetos viejos. Ninguna WLPN de la muestra es Tipo I. Así, [WR]PNe y WLPNe no están relacionados.

ABSTRACT

High resolution spectra are used to analyze the galactic kinematics and distribution of a sample of planetary nebulae with [WR] and ‘wel’ central star ([WR]PN and WLPN). The circular and peculiar velocities, (V_{pec}), of the objects were derived. The results are: (a) [WR]PNe are distributed mainly in the galactic disk and they are more concentrated in a thinner disk than WLPNe and normal PNe, which corresponds to a younger population. (b) The sample was separated in Peimbert’s types, and it is found that Type I PNe have $V_{\text{pec}} \leq 50 \text{ km s}^{-1}$, indicating young objects. Most of the [WR]PNe are of Type II showing $V_{\text{pec}} \leq 60 \text{ km s}^{-1}$, although a small percentage is of Type III with larger V_{pec} . This shows that the Wolf-Rayet phenomenon in central stars can occur at any stellar mass and in old objects. None of our WLPNe is of Type I. Thus, [WR]PNe and WLPNe are unrelated objects.

Key Words: planetary nebulae: general — stars: kinematics and dynamics — stars: Wolf-Rayet

1. INTRODUCTION

Planetary nebulae (PNe) are formed from highly evolved low-medium mass stars, which are in the pre-white dwarf stage. The age of PN central stars fluctuates between 0.1 to about 9 Gyr (Allen, Carigi, & Peimbert 1998). The chemical abundances in the nebulae are typical of the moment when the star was

born, except for some elements like He, N, C, and possibly O, which have been processed in the stellar nucleus and have been partially dredged up to the surface through several dredge-up events. Thus, the youngest PNe show O, Ne, Ar, S and other α -element abundances similar to those of the present interstellar medium, while the older objects show abundances typical of an older stellar population. Also the galactic kinematics is different in the sense that the young objects belong to the thin disk, while the oldest PNe belong to the galactic halo and appear as high velocity objects. In general most of the PNe are intermediate disk population. See Peimbert (1978, 1990) for a thorough review on these subjects.

¹Based on observations collected at the Observatorio Astronómico Nacional, SPM, B. C., Mexico. Based on data obtained at Las Campanas Observatory, Carnegie Institution, Chile.

²Instituto de Astronomía, Universidad Nacional Autónoma de México, Mexico.

³Instituto de Astrofísica de Canarias, Spain.

⁴Departamento de Astrofísica, Universidad de La Laguna, Spain.

Considering the above, Peimbert (1978) classified the galactic PNe in four types, according to their chemical composition and kinematics (see also Peimbert & Serrano 1980, and Peimbert & Torres-Peimbert 1983). According to Peimbert (1990), who presents a more refined classification, the main characteristics of the different types are: Type I PNe are He- and N-rich objects ($\text{He}/\text{H} \geq 0.125$, $\text{N}/\text{O} \geq 0.5$), the initial masses of their central stars are in the range $2 - 8 M_{\odot}$, the nebulae have, in general, bipolar morphologies, and they belong to the young population; Type II PNe, representing the majority of the known PN sample, are intermediate population, they have no particular He and N enrichment, the initial masses of their central stars are smaller than $2 M_{\odot}$ and they show peculiar velocities smaller than 60 km s^{-1} ; Type III PNe are similar to Type IIs, but their peculiar velocities are larger than 60 km s^{-1} and they probably have distances to the galactic plane larger than 1 kpc. Finally, Type IV PNe are defined as those extreme Population II objects that belong to the galactic halo; there are only a few objects in this category and they show very low metallicities and high peculiar velocities (see e.g., Howard, Henry, & McCartney 1997). Peimbert's classification has been revised by several authors. It is worth to mention for instance, that Kingsburgh & Barlow (1994) proposed as Type I those object with $\text{N}/\text{O} \geq 0.8$. In § 4 we will use some of the criteria given above for classifying our objects.

Among central stars of PNe there is a particular group which presents important atmospheric instabilities and large mass losses. Their spectra are similar to the ones shown by massive Wolf-Rayet stars of the C series and are classified in a similar way but with the nomenclature [WC] or [WO]. PNe with this type of star represent no more than 15% of the known sample and in the following we will call them [WR]PNe. The [WR] central stars are H-deficient and their atmospheres show He, C and O, a composition typical of the zone where nucleosynthesis took place (e.g., Koesterke 2001). Many studies have been devoted to analyze this special type of central stars and their surrounding nebulae (e.g., Górny & Stasińska 1995; Peña, Stasińska, & Medina 2001; Gesicki et al. 2006; Górny et al. 2009; García-Rojas, Peña, & Peimbert 2009; García-Rojas et al. 2012; DePew et al. 2011, among others).

In this paper we analyze high spectral resolution data obtained with the 2.1-m telescope and the Echelle REOSC spectrograph of the Observatorio Astronómico Nacional San Pedro Mártir (OAN-SPM), México, and with the 6.5-m Clay Tele-

scope equipped with the double echelle spectrograph MIKE, at Las Campanas Observatory (LCO), Chile, in order to study the galactic kinematical behavior of nearly a hundred PNe. Of these, a significant number are [WR]PNe and the rest are ionized by normal central stars or by weak emission-line stars (wels)

In § 2 we present the PN sample, the observations and the Galactic distribution of the objects; in § 3, the heliocentric, circular and peculiar velocities are calculated for the sample with available distances. The distribution of objects in the different Peimbert Types is presented and discussed in § 4, and our conclusions can be found in § 5.

2. THE SAMPLE: OBSERVATIONS AND DATA ANALYSIS AND THE GALACTIC DISTRIBUTION OF OBJECTS.

The log of our observations, for the whole sample, is presented in Table 1, where we list the observatory and the observing date for each object. The sample collected at the OAN-SPM consists of 56 PNe observed from 1995 to 2001, while the sample from LCO (Clay telescope) consists of 25 objects (9 are in common with the OAN-SPM sample), observed during runs in 2006, 2009 and 2010.

For the SPM objects, the echelle spectrograph REOSC was used at high resolution (Levine & Chakrabarty 1994). The observed wavelength range covers from about 3600 to 6900 Å. The description of the observations as well as the data reduction procedure can be found in Peña et al. (2001) and Medina et al. (2006). In these works, the data of a sample of objects from Table 1 (mainly [WR]PNe), were used to derive and analyze the physical conditions, chemical abundances, and expansion velocities of the nebulae. In this paper we use the data presented in those works (notice that several nebulae were observed more than once, and here we are using only one spectrum for radial velocities measurements), together with data for other objects (processed in the same way) to derive radial velocities of the nebulae. The spectral resolution of these spectra is 0.2 to 0.3 Å per pix which allows us to determine radial velocities with a precision of about 12 to 19 km s^{-1} .

The data for LCO objects were obtained with the double echelle Magellan Inamori Kyocera spectrograph, MIKE (Berstein et al. 2003). A full description of the observations and data reduction procedures is presented by García-Rojas et al. (2009) and García-Rojas et al. (2012), who have used the data of thirteen of these objects to analyze the physical conditions and chemical behavior of the nebulae. In this case the spectral resolution is better than

TABLE 1
LOG OF OBSERVATIONS¹

PN G	Name	Obs.	Obs. date ²	PN G	Name	Obs.	Obs. date ²
001.5–06.7	SwSt1*	LCO	08/09/09	103.7+00.4	M2-52*	SPM	02/11/00
001.5–06.7	"	SPM	05/08/97	104.4–01.6	M2-53*	SPM	02/11/00
002.2–09.4	Cn1-5*	LCO	09/09/09	108.4–76.1	BoBn1*	SPM	27/08/01
002.2–09.4	"	SPM	17/06/96	111.8–02.8	Hb12*	SPM	25/08/01
002.4+05.8	NGC 6369*	LCO	05/06/10	118.0–08.6	Vy1-1*	SPM	02/11/00
002.4+05.8	"	SPM	15/06/96	118.8–74.7	NGC 246*	SPM	13/12/98
003.1+02.9	Hb4*	LCO	05/06/10	119.6–06.7	Hu1-1*	SPM	26/08/01
003.1+02.9	"	SPM	14/06/96	120.0+09.8	NGC 40*	SPM	13/12/98
003.9-14.9	Hb7*	SPM	26/08/01	130.2+01.3	IC 1747*	SPM	14/12/98
004.9+04.9	M1-25	LCO	05/06/10	130.3–11.7	M1-1*	SPM	02/11/00
004.9+04.9	"	SPM	17/06/96	130.9–10.5	NGC 650-51*	SPM	26/08/01
006.8+04.1	M3-15*	LCO	08/09/09	133.1–08.6	M1-2*	SPM	27/08/01
006.8+04.1	"	SPM	17/06/96	144.5+06.5	NGC 1501	SPM	14/12/98
009.4–05.5	NGC 6629*	SPM	05/08/97	146.7+07.6	M4-18*	SPM	14/12/98
010.8–01.8	NGC 6578	SPM	14/06/96	159.0–15.1	IC 351*	SPM	05/10/99
011.7–00.6	NGC 6567*	SPM	05/08/97	161.2–14.8	IC 2003*	SPM	05/10/99
011.9+04.2	M1-32*	LCO	05/06/10	166.1+10.4	IC 2149*	SPM	14/12/98
011.9+04.2	"	SPM	14/06/96	194.2+02.5	J900*	SPM	02/11/00
012.2+04.9	PM1-188	SPM	04/08/97	197.8+17.3	NGC 2392*	SPM	13/12/98
017.9–04.8	M3-30*	SPM	17/06/96	243.3–01.0	NGC 2452*	SPM	13/12/98
019.4–05.3	M1-61	LCO	05/06/10	278.1–05.9	NGC 2867	LCO	08/05/06
019.4–05.3	"	SPM	25/08/01	278.8+04.9	PB6	LCO	10/05/06
019.7–04.5	M1-60	SPM	25/08/01	285.4+01.5	Pe1-1	LCO	04/06/10
025.8–17.9	NGC 6818*	SPM	27/08/01	286.3+02.8	He2-55	LCO	10/05/06
027.6+04.2	M2-43	SPM	17/06/96	291.3–26.2	Vo1	LCO	08/05/06
029.2–05.9	NGC 6751*	LCO	09/09/09	292.4+04.1	PB8	LCO	09/05/06
037.7–34.5	NGC 7009*	SPM	02/11/01	294.1+43.6	NGC 4361*	SPM	17/06/96
042.5–14.5	NGC 6852*	SPM	27/08/01	300.7–02.0	He2-86	LCO	05/06/10
046.4–04.1	NGC 6803*	SPM	26/08/01	307.2–03.4	NGC 5189*	LCO	09/05/06
048.7+01.9	He2-429	SPM	05/10/99	309.0–04.2	He2-99	LCO	09/05/06
051.9–03.8	M1-73	SPM	26/08/01	321.0+03.9	He2-113	LCO	09/05/06
054.1–12.1	NGC 6891*	SPM	25/08/01	327.1–02.2	He2-142	LCO	09/05/06
058.3–10.9	IC 4997*	SPM	25/08/01	332.9–09.9	CPD-56	LCO	10/05/06
061.4–09.5	NGC 6905*	SPM	14/06/96	336.2–06.9	PC14	LCO	05/06/10
064.7+05.0	BD+30 3639*	SPM	05/10/99	337.4+01.6	Pe1-7	LCO	04/06/10
086.5–08.8	Hu1-2*	SPM	25/08/01	355.2–02.5	H1-29	SPM	26/08/01
089.0+00.3	NGC 7026*	SPM	14/12/98	355.9–04.2	M1-30*	LCO	05/06/10
089.8–05.1	IC 5117*	SPM	25/08/01	355.9–04.2	"	SPM	27/08/01
096.3+02.3	K3-61*	SPM	05/10/99	356.2–04.4	Cn2-1*	SPM	05/08/97
096.4+29.9	NGC 6543*	SPM	15/06/96	358.3–21.6	IC 1297	LCO	08/09/09
100.6–05.4	IC 5217*	SPM	05/10/99				

¹The observatory and observing dates are indicated. Observations at LCO were obtained with MIKE, and at SPM, with the echelle REOSC. Objects with * are part of the sample downloaded from the SPM Kinematic Catalogue.

²Observing date in dd/mm/yy.

0.17 Å in the blue (about 10.8 km s⁻¹) and 0.23 in the red (about 12.8 km s⁻¹).

In addition, we have collected data from the SPM Kinematic Catalogue of Galactic Planetary Nebulae (López et al. 2012), which provides spatially resolved, long-slit echelle spectra for about 600 galactic PNe. Position-velocity images in H α , [NII] $\lambda\lambda$ 6548, 6583, and [OIII] λ 5007, obtained with different slit positions across the nebulae, are presented for each object. From this catalogue, we downloaded all the available spectra of [WR]PNe (slit passing through the center), in order to measure their systemic heliocentric radial velocity. In total we found 54 objects. Of these, 48 are in common with SPM and LCO objects (they are marked with * in Table 1). The additional 6 objects, not observed at SPM or LCO, are PN G009.8-04.6, PN G068.3-02.7, PN G081.2-14.9, PN G189.1+19.8, PN G208.5+33.2, and PN G307.5-04.9.

Our final sample, with measured radial velocities, consists of 78 objects of which 44 are [WR]PNe, 3 are [WC]-PG1159 objects (considered as one group in the following), and 16 PNe are ionized by wels (hereafter WLPNe). The remaining 15 PNe contain a normal or a PG1159 central star. The [WR]PN sample represents 43% of the total sample of known [WR]PNe which presently amounts to 103 objects (De Pew et al. 2011). Medina et al. (2006) showed that, regarding the expansion velocities, WLPNe behave similarly to normal PNe. Gesicki et al. (2006) and other authors found that there are noticeable differences between [WR]PNe and WLPNe, so in the following, we will consider WLPNe and normal PNe in one group, apart from the [WR]PN group. This will be further discussed in § 2.1 and § 4.

Since we are analyzing the distribution and galactic kinematics of [WR]PNe, we have included in our sample another five [WR]PNe (PN G020.9-01.1, PN G274.3+09.1, PN G306.422.4-00.1, PN G309.1-04.3, and PN G322.4-00.1) for which we found distances (given by Stanghellini & Haywood 2010), but no velocities. They will be used for analyzing the galactic distribution of [WR]PNe.

The main characteristics of all the analyzed objects are presented in Table 4 where we include, in Column 1, the name corresponding to the Strasbourg-ESO Catalogue of Galactic Planetary Nebulae by Acker et al. (1992); in Column 2, the common name and, in Column 3, the spectral classification of the central star: [WC#] or [WO#] for Wolf-Rayet central stars, ‘wels’ for weak emission line stars, and ‘pn’ for normal stars. The [WR] or ‘wels’ classifications were adopted from Acker &

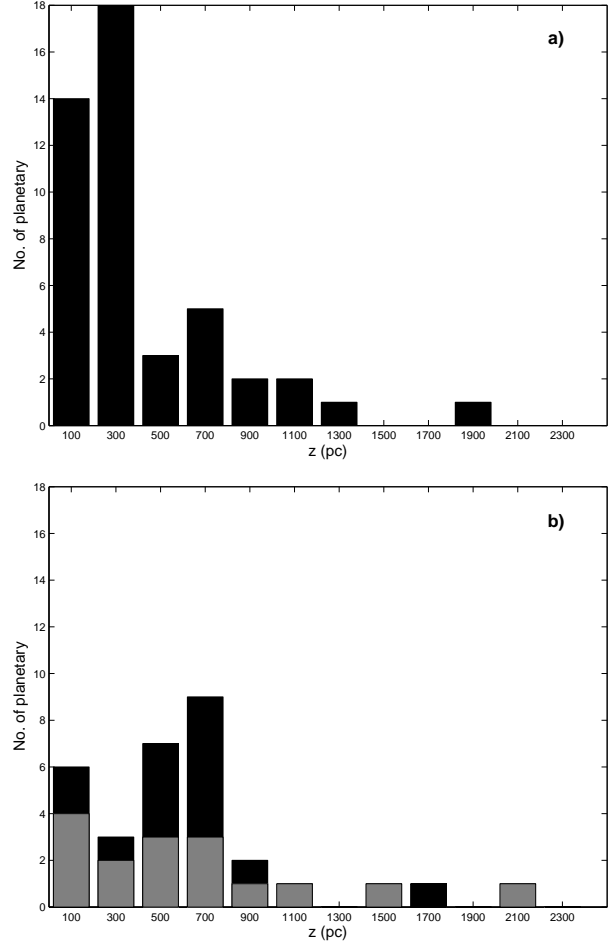


Fig. 1. Distribution of objects at different height, z , above the galactic plane. (a) [WR]PNe (46 objects), (b) objects ionized by wels (histogram in gray) and by normal central stars (histogram in black); 31 objects in total. The halo PN G108.4-76.1 (BoBn 1) is not represented here. It has $z = 17$ kpc.

Neiner (2003, and references therein), and Todt et al. (2010) for the case of PN G292.4+04.1 (PB 8). Columns 4 and 5 of Table 4 show the galactocentric distances of the objects and their errors, as given in the work by Stanghellini & Haywood (2010).

2.1. Distribution of [WR]PNe and WLPNe, relative to the galactic disk

Figure 1 presents the distribution of objects ([WR]PNe, WLPNe and normal PNe as a function of height above the galactic disk, z (pc). Heights were obtained by assuming the heliocentric distances given by Stanghellini & Haywood (2010, distances were found for 78 objects) and taking into account the galactic coordinates of the objects. The heights are listed in Column 6 of Table 4. In the graph

for [WR]PNe (Figure 1a, which also includes three [WC]-PG1159 stars) it is evident that most of the objects (32 of 46) belong to a thin disk with height smaller than 400 pc, while in the graph for WLPNe and normal PNe (Figure 1b), the great majority of the objects (25 of 31) have heights above the galactic plane of up to 800 pc. It is very interesting to notice that WLPNe (gray histogram in Figure 1b) do not show any particular concentration towards the thin disk. Twelve of sixteen WLPNe have heights up to 800 pc and the other four objects are located at larger z , very similar to the distribution shown by PNe with normal central stars. Although there are only 16 WLPNe in our sample, this result indicates that these objects are distributed differently than [WR]PNe.

Thus, regarding their position in the Galaxy, [WR]PNe seem to belong to a population located in a thinner disk than PNe ionized by wels and normal central stars, indicating that progenitor stars of [WR]PNe would be younger and with larger initial masses (similar results were found by Weidmann & Gamen 2011 for their sample of H-poor central stars). In our [WR]PN sample there are only 4 objects with $z > 1$ kpc; they are PN G358.3-21.6 (IC 1297) with $z = 1.827$ kpc, PN G161.2-14.8 (IC 2003) with $z = 1.21$ kpc, PN G146.7+0.6 (M 4-18) with $z = 1.185$ kpc, and PN G118.0-08.6 (Vy 1-1) with $z = 1.07$ kpc.

The galactic distribution of [WR]PNe was previously analyzed by Acker, Górný, & Cuisinier (1996). They found that the fraction of [WR]PNe with galactic latitude $|b| < 7^\circ$ is similar to the fraction for normal PNe, thus concluding that both distributions are equal. However, they did not consider the distances and heights above the galactic plane, which is probably the reason for the difference between their and our results.

3. HELIOCENTRIC, CIRCULAR AND PECULIAR RADIAL VELOCITIES

For the objects observed at the OAN-SPM and LCO, radial velocities were measured from the most intense spectral lines (not saturated), such as [OIII] $\lambda\lambda$ 5007, 4959, H γ , H β , H α , [NII] $\lambda\lambda$ 6548, 6583, by using the task `SPLOT` of IRAF⁵.

For the OAN-SPM data we found that the red zone of our spectra (wavelength longer than 6000 Å) was not properly calibrated in wavelength, giving results with large discrepancies relative to the

blue zone, therefore we used only the blue lines [OIII] $\lambda\lambda$ 5007, 4959, H γ , and H β to determine the radial velocities of these objects. The data from LCO have better resolution and the blue and red lines show almost no discrepancy; therefore radial velocities were measured for all the lines, (and their results are preferred over those in the OAN-SPM and SPM kinematical catalogue).

The finally adopted radial velocity in each case, corresponds to the average obtained from the used lines and the errors were calculated as the mean quadratic error, $\Delta V = (\sum_i (V_i - V)^2 / (n(n-1)))^{1/2}$, where V_i is the velocity for each line, V is the average velocity and n is the number of considered lines. Then, these errors represent the internal consistency of our spectra and not necessarily the true uncertainty in the determined velocity (see § 3.1).

Afterwards we used the IRAF routine `RVCORRECT` to determine, for each object, the heliocentric radial velocity and its error. The results are presented in Columns 7 and 8 of Table 4. In these columns, the data from LCO are boldfaced.

As said before, we selected the galactic disk [WR]PNe, appearing in the Kinematical Catalogue of SPM (López et al. 2012) and determined the heliocentric radial velocities of these objects by measuring the systemic velocity of the nebula from the position-velocity diagram obtained when the slit was positioned through the center of the object. We measured all the available lines for each object ([OIII] λ 5007, H α , and [NII] $\lambda\lambda$ 6548, 6583). Such velocities, V_{Cat} , are listed in Column 9 of Table 4. Notice that for a few objects this is the only available velocity.

3.1. Analysis of velocities

An adequate way of estimating the uncertainties in an observed quantity is by comparing independent measurements of the quantity. For the heliocentric velocities of our objects we have, in most of the cases, two or three independent observations that can be compared, and thus the uncertainties can be estimated.

Figure 2 shows a comparison of our heliocentric radial velocities (V_{LCO} and V_{SPM}) with the values derived from the SPM Kinematical Catalogue, (V_{Cat}), and with values from the literature (Durrand, Acker, & Zijlstra 1998, V_{DAZ}). A 45° slope line has been included in all the graphs for comparison. It is evident that the velocities from LCO and from the Kinematical Catalogue (Figure 2, top left), which are the ones with the best spectral resolution, are very well correlated; the linear correlation is

⁵IRAF is distributed by the National Optical Astronomy Observatories, which is operated by the Association of Universities for Research in Astronomy, Inc. (AURA) under contract with the National Science Foundation.

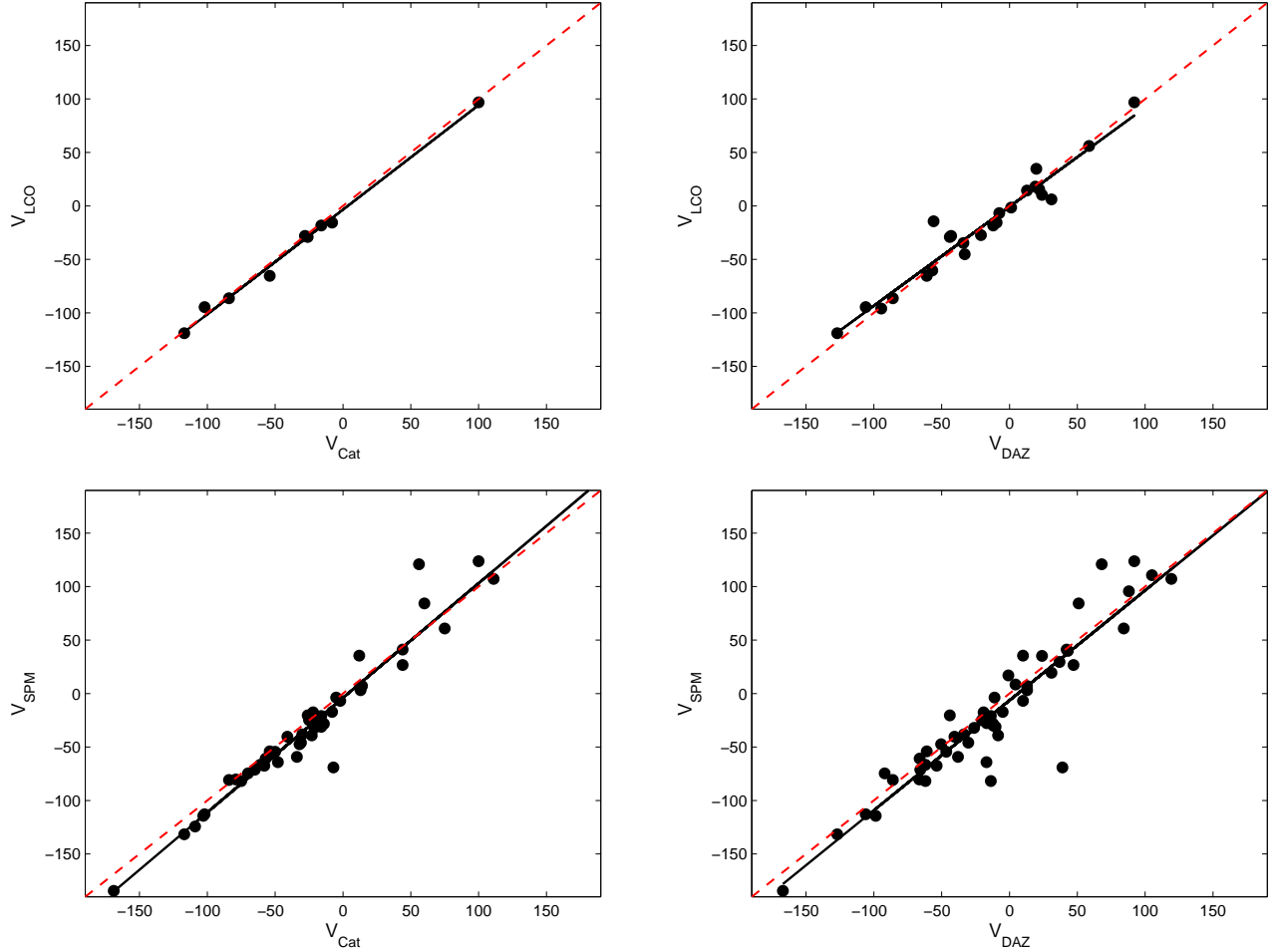


Fig. 2. Comparison of heliocentric radial velocities from different observations. Top: V_{LCO} vs. velocities from the SPM Kinematical Catalog, V_{Cat} , and V_{LCO} vs. Durand et al. (DAZ, 1998) data. Bottom: V_{SPM} vs. V_{Cat} and V_{SPM} vs. Durand et al. (1998) velocities. The solid lines represent the linear fits to the data and they are discussed in the text. The dashes lines represent a 1:1 relation (45° slope lines).

$V_{\text{LCO}} = 0.978 V_{\text{Cat}} - 3.543 \text{ km s}^{-1}$, with a correlation coefficient $r^2 = 0.994$. The dispersion of the differences ($V_{\text{LCO}} - V_{\text{Cat}}$) is 3.8 km s^{-1} . For the velocities from SPM we found a good correlation with those from the Kinematical Catalogue (Figure 2, bottom left), except for a few objects showing large differences. The linear fit is $V_{\text{SPM}} = 1.072 V_{\text{Cat}} - 3.967$, with $r^2 = 0.948$. The dispersion of the differences ($V_{\text{SPM}} - V_{\text{Cat}}$) is 12.9 km s^{-1} .

The comparison of V_{LCO} vs. V_{DAZ} (Figure 2, top right) is also good with only one object showing a discrepancy as large as 40 km s^{-1} . The fit is $V_{\text{LCO}} = 0.927 V_{\text{DAZ}} - 0.719$ with correlation coefficient $r^2 = 0.942$. The dispersion of the differences ($V_{\text{LCO}} - V_{\text{DAZ}}$) is 8.8 km s^{-1} . The correlation is worse for V_{SPM} vs. V_{DAZ} data (Figure 2, bottom right); it has a fit $V_{\text{SPM}} = 1.028 V_{\text{DAZ}} - 6.382$, with

correlation coefficient $r^2 = 0.890$. The dispersion of the differences is, in this case, 18.0 km s^{-1} . Durand et al. (1998) data correspond to a compilation from the literature of results from different authors and, according to these authors, most of their sample presents velocity uncertainties better than about 20 km s^{-1} .

In all the graphs it is apparent that the 1:1 correlation and the linear fits are very similar, showing the good quality of the different estimates of velocities.

Considering the above discussion, we decided to adopt, when possible, the velocities obtained from LCO with an uncertainty of $\pm 3.8 \text{ km s}^{-1}$; if these were not available, we adopted the velocities from the SPM Kinematical Catalogue with the same uncertainty and, as a third choice, we used the veloc-

TABLE 2
KINEMATICAL PARAMETERS FOR
EQUATION 1

Parameter	Value (units)	Ref. ¹
u_{\odot}	10.4 (km s ⁻¹)	1
v_{\odot}	14.8 (km s ⁻¹)	1
w_{\odot}	7.3 (km s ⁻¹)	1
R_{\odot}	8.0±0.5 (kpc)	2
A	14.4±1.2 (km s ⁻¹ kpc ⁻¹)	3
A_2	13.0±0.9 (km s ⁻¹ kpc ⁻²)	4
K	5.1±2.8 (km s ⁻¹)	4

¹1. Mihalas & Routly 1968; 2. Reid 1993; 3. Kerr & Lynden-Bell 1986; 4. Durand et al. 1998.

ities obtained with the Echelle REOSC from SPM, assuming an uncertainty of ±12.9 km s⁻¹.

3.2. Circular velocities

From the galactocentric distance of the objects, R_G , as given by Stanghellini & Haywood (2010), we determined their circular radial velocities following the expression:

$$V_{\text{circ}} = -u_{\odot} \cos l \cos b - v_{\odot} \sin l \cos b - w_{\odot} \sin b - 2A(R_G - R_{\odot}) \sin l \cos b + \frac{A_2}{2} (R_G - R_{\odot})^2 \sin l \cos b + K. \quad (1)$$

This equation is the expansion to second order of the circular radial velocity as a function of R_G . The expansion to second order allows us to use the kinematics of objects located further from the Sun. In equation 1, u_{\odot} , v_{\odot} and w_{\odot} are the radial, azimuthal and vertical components of the solar motion relative to the Local Standard of Rest. R_{\odot} is the distance of the Sun to the galactic center and l and b are the galactic longitude and latitude of the object.

The forth term on the right side of equation 1 represents the usual differential galactic rotation to first order, A being the Oort constant. In the second row, A_2 is the second order coefficient of the derivative of the rotation speed with respect to R_G , and K is the K -term of local galactic expansion.

To calculate the radial circular velocities from equation 1, we used the standard values for the kinematical parameters listed in Table 2.

Values for the derived V_{circ} are listed in Column 11 of Table 4. The errors for V_{circ} (Columns 12 and 13) were computed by considering the errors in the galactocentric distances.

After calculating V_{circ} we determined the peculiar velocity for each object as:

$$V_{\text{pec}} = V_{\text{hel}} - V_{\text{circ}}.$$

The resulting values and the corresponding errors are listed in Columns 14, 15, and 16 of Table 4. It is important to notice that the errors in the distances are, in general, the most important uncertainties in computing V_{pec} .

4. STELLAR POPULATIONS OF PNE

We have classified our sample of PNe using the criteria of Peimbert's classification scheme defined in § 1; thus Type I are the PNe with He/H>0.125, and N/O>0.5, Type II do not show He or N enrichment and have $V_{\text{pec}} \leq 60$ km s⁻¹ and Type III have $V_{\text{pec}} > 60$ km s⁻¹. The chemical composition for our objects (important for Type I classification) was adopted from the works by García-Rojas et al. (2009, 2013, in preparation), Peña et al. (2001) or from the literature. For each Type I object we have listed its relevant abundance ratios (N/O and He/H) in Table 3, where the source for abundances is identified.

Peimbert's type for each object is shown in Column 17 of Table 4. In Table 5 we present a summary of the number of [WR]PNe, WLPNe and normal PNe in each type. In next subsections a discussion on the different Peimbert type samples is given.

4.1. Type I objects

As expected, Type I PNe show, in general, low peculiar velocities (smaller than 50 km s⁻¹). This agrees with these PNe being supposedly produced by the most massive stars among progenitors ($M_i \geq 2.0 M_{\odot}$, Peimbert & Serrano 1980).

In our [WR]PN+[WR]-PG1159 sample, there are 10 Type I PNe and among them there are two objects with high peculiar velocities: PN G003.1+02.9 (Hb 4) with $V_{\text{pec}} = -75.9$ km s⁻¹, and PN G011.9+04.2 (M1-32), with $V_{\text{pec}} = -132.2$. If we follow the standard criteria for considering an object as belonging to the bulge, which are: galactic position within 10° from the galactic center, radius smaller than 20'' and radio flux at 5 GHz smaller than 100 mJy (Stasińska & Tyłenda 1994; Cavichia, Costa, & Maciel 2011), Hb 4 could be considered as belonging to the bulge, because it is located within 10° from the galactic center, it has a radius of 2.5'' and its flux at 5 GHz (6 cm) is 166 mJy. Then, Hb 4 fulfills all the criteria except that it is brighter at 5 GHz. Its galactocentric distance is

TABLE 3
PEIMBERT'S TYPE I PNE ([WR]PNE ARE BOLDFACED)

	Object	V_{pec}	N/O	He/H	Ref. ¹
001.5–06.7	SwSt 1	–17.0	0.80	0.040	PSM01
002.2–09.4	Cn 1-5	–37.9	0.83	0.158	G-R12
003.1+02.9	Hb 4	–75.9	0.71	0.115	G-R12
011.9+04.2	M 1-32	–132.3	0.51	0.126	G-R12
064.7+05.0	BD+30 3036	–40.5	1.25	—	PSM01
086.5–08.8	Hu 1-2	19.0	1.15	0.151	PLT-P95
089.0+00.3	NGC 7026	–24.8	1.01	0.124	PSM01
103.7+00.4	M 2-52	–32.3	2.3	0.165	PM02
278.8+04.9	PB 6	25.1	1.48	0.19	G-R09
300.7–02.0	He 2-86	5.9	0.72	0.123	G-R12
307.2–03.4	NGC 5189	–16.9	0.68	0.123	KB94
307.5–04.9	MyCn 18	–34.6	1.04	0.095	KB94

¹PSM01: Peña et al. 2001; G-R12: García-Rojas et al. 2013 in prep; PLT-P95: Peimbert, Luridiana, & Torres-Peimbert 1995; PM02: Peña & Medina 2002; G-R09: García-Rojas et al. 2009; KB94: Kingsburgh & Barlow 1994.

about 2.9 ± 1.0 kpc, so it could be part of the bulge, despite its relatively strong 5 GHz flux.

M 1-32 is a peculiar object. Its chemical abundances (N/O=0.51 and He/H=0.126) locate it marginally among Type I PNe. If Kingsburgh & Barlow (1994) criteria were adopted, it would not be a Type I PN and its peculiar velocity would locate it among Type III's despite its height above the galactic plane being only 0.35 kpc. The internal kinematics of M 1-32 is peculiar; Medina et al. (2006) found high velocity wings in the nebular lines, which are also apparent in Figure 1 of García-Rojas et al. (2012). Recently Akras & López (2012) analyzed the velocity field in this object and confirmed the high velocity wings, which they interpret as due to collimated bipolar outflows reaching velocities of ± 200 km s⁻¹. These authors consider M 1-32 as a bulge object. Its angular diameter is 7.6'' and its observed flux at 5 GHz is 61 mJy, so these two criteria are fulfilled for being a bulge PN. However it is located at more than 10° from the galactic center, at a galactocentric distance of about 3.46 ± 0.84 kpc. With these characteristics M 1-32 could be at the border of the bulge and its high V_{pec} could be a consequence of its location in the Galaxy.

Regarding WLPNe, it is important to remark that none of the objects in our sample is a Type I PN. This fact was already mentioned by Peña, Medina, & Stasińska (2003) for a smaller sample, and also by Fogel, De Marco, & Jacoby (2003), who an-

alyzed a sample of 42 WLPNe finding none of Type I among them.

Our sample includes only a small number (12) of normal PNe chosen randomly (11 objects belong to the disk and one to the galactic halo), which is by no means representative of the total galactic PNe. In this short sample we have 2 Type I PNe (17%), a fraction similar to that found in larger samples (e.g., Peimbert 1990).

4.2. Type II objects

Among the [WR]PNe and [WC]-PG1159 PNe, there are 23 objects (51% of the sample) classified as Type II. This also occurs among normal PNe, where the Type II objects are the majority (see e.g., Peimbert 1990; Stanghellini & Haywood 2010). Among our normal PN and WLPN samples, there are 6 and 7 Type II PNe, respectively. These PNe belong to the intermediate disk population, their progenitors had initial masses smaller than $2 M_{\odot}$, and in consequence they would be older than Type I objects.

4.3. Type III objects

Interestingly, there are five [WR]PNe among the Type III objects which, as we said, have V_{pec} larger than 60 km s⁻¹ and are the older PNe among the disk population, belonging probably to the thick disk. The five objects represent 11.6% of our [WR] sample; they are PNG 002.4+5.8 (NGC 6369, [WC]4,

TABLE 4
 MAIN CHARACTERISTICS, HELIOCENTRIC, CIRCULAR AND PECULIAR VELOCITIES OF ANALYZED OBJECTS

PN G	Name	Spectral type	R_G kpc	ΔR_G kpc	z pc	V_{hel}^a km s ⁻¹	ΔV_{hel} km s ⁻¹	V_{Cat} km s ⁻¹	ΔV_{Cat} km s ⁻¹	V_{circ} km s ⁻¹	$\Delta V_{circ}(-)$ km s ⁻¹	$\Delta V_{circ}(+)$ km s ⁻¹	V_{pec} km s ⁻¹	$\Delta V_{pec}(+)$ km s ⁻¹	$\Delta V_{pec}(-)$ km s ⁻¹	Peimbert Type
001.5-06.7	Swst 1	[WC9]pec	5.17	0.57	332.9	-18.3	0.4	-16.0	2.0	-1.3	-1.0	+1.1	-17.0	+4.9	-4.8	I
002.2-09.4	Cn 1-5	[WO4]pec	2.50	1.09	912.0	-29.9	2.5	-26.0	2.0	8.9	-4.2	+4.7	-37.9	+8.5	-8.0	bulge
002.4+05.8	NGC 6369	[WO3]	6.91	0.22	111.4	-94.6	3.2	-102.0	1.0	-5.0	-0.4	+0.5	-89.6	+4.3	-4.2	III
003.1+02.9	Hb 4	[WO3]	2.93	1.01	257.8	-112.9	0.8	-54.0	2.0	10.5	-5.1	+5.9	-75.9	+9.7	-8.9	I, bulge?
003.9-14.9	Hb 7	wels	0.55	0.16	2109.3	-66.6	4.3	-61.0	2.0	33.8	-1.4	+1.3	-94.8	+5.1	-5.2	III
004.9+04.9	M 1-25	[WC5-6]	1.48	1.18	571.0	10.3	0.7	32.4	-11.2	+12.9	-22.1	+16.7	-15.0	bulge
006.8+04.1	M 3-15	[WC4]	1.48	1.05	106.0	96.9	0.8	100.0	1.0	47.4	-14.0	+15.6	49.5	+19.4	-17.8	bulge
009.4-05.5	NGC 6629	[WC4]	5.66	0.47	229.9	3.2	2.6	13.0	1.0	10.0	-4.7	+5.2	3.0	+9.0	-8.5	II
009.8-04.6	H 1-67	[WR]	1.36	0.06	630.4	-15.0	2.0	74.0	-1.1	+1.1	-89.0	+4.9	-4.9	bulge
010.8-01.8	NGC 6578	wels	4.44	0.69	115.6	8.5	1.7	27.0	-10.0	+11.2	-18.5	+24.1	-22.9	II
011.7-00.6	NGC 6567	wels	4.49	0.68	38.2	107.2	4.5	111.0	1.0	28.8	-10.6	+11.8	82.2	+15.6	-14.4	III
011.9+04.2	M 1-32	[WO4]pec	3.46	0.84	351.3	-86.4	0.8	-84.0	2.0	45.8	-15.3	+17.3	-132.2	+21.1	-19.1	I, bulge?
012.2+04.9	PM 1-188	[WC10]	39.9	3.0
017.9-04.8	M 3-30	[WO2]	3.95	0.71	379.6	84.3	2.4	60.0	2.0	59.7	-18.0	+20.1	0.3	+23.9	-21.8	II
019.4-05.3	M 1-61	wels	3.43	0.68	498.4	6.1	0.5	79.5	-20.3	+22.3	-73.4	+26.1	-24.1	III
019.7-04.5	M 1-50	[WC4]	3.33	1.11	746.6	95.6	1.3	83.8	-33.2	+38.6	11.8	+51.5	-46.1	II
020.9-01.1	M 1-51	[WO4]pec	5.89	0.40	44.6
025.8-17.9	NGC 6818	wels	6.28	0.33	639.0	-21.0	2.7	-16.0	2.0	20.8	-7.6	+10.3	-36.8	+14.1	-11.4	II
027.6+04.2	M 2-43	[WC7-8]	5.37	0.46	235.5	110.6	1.1	44.4	-14.3	+15.5	66.2	+28.4	-23.7	II
029.2-05.9	NGC 6751	[WO4]	5.84	0.39	272.7	-28.0	0.6	-28.0	1.0	34.5	-11.6	+12.6	-62.5	+15.4	-13.1	III
037.7-34.5	NGC 7009	pn	7.14	0.17	779.4	-54.4	3.5	-50.0	1.0	10.0	-3.8	+4	-60.0	+7.8	-7.6	III
042.5-14.5	NGC 6852	PG1159	6.29	0.27	693.1	-3.7	1.2	-5.0	2.0	34.5	-10.0	+10.7	-39.5	+14.5	-13.8	II
046.4-04.1	NGC 6803	wels	5.80	0.04	381.4	7.1	3.3	14.0	2.0	56.4	-1.6	+1.7	-42.4	+5.5	-5.4	II
048.7+01.9	He 2-429	[WC4]	6.18	0.32	223.3	17.0	3.9	42.3	-13.5	+14.5	-25.3	+27.4	-26.5	II
051.9-03.8	M 1-73	wels	6.53	0.35	442.4	-81.8	2.2	31.9	-14.4	+15.7	-113.7	+28.6	-27.3	III
054.1-12.1	NGC 6891	wels	6.74	0.16	607.9	41.1	3.4	44.0	1.0	25.8	-6.3	+6.5	18.2	+10.4	-10.1	II
058.3-10.9	IC 4997	wels	7.02	0.29	1142.3	-60.8	2.0	-57.0	3.0	17.5	-11.3	+12.2	-74.5	+16.0	-15.1	III
061.4-09.5	NGC 6905	[WO2]	7.32	0.10	294.1	-39.1	5.6	-23.0	1.0	8.0	-3.7	+3.9	-31.0	+7.7	-7.5	II
064.7+05.0	BD+30o 3639	[WC9]	7.25	0.04	257.6	-45.9	3.0	-31.0	2.0	9.5	-1.6	+1.5	-40.5	+5.3	-5.4	I
068.3-02.7	He 2-459	[WC9]	9.12	0.96	388.7	-38.0	2.0	-34.5	-12.9	+23.9	-3.5	+27.7	-16.7	II
081.2-14.9	A 78	[WC]-PG1159	7.91	0.01	421.7	-20.0	2.0	-6.3	-0.5	+0.5	-13.7	+4.4	-4.4	I
086.5-08.8	Hu 1-2	pn	8.47	0.22	513.3	-6.9	2.3	-2.0	1.0	-21.0	-6.0	+6.7	19.0	+10.5	-9.8	I
089.0+00.3	NGC 7026	[WO3]	8.23	0.10	10.9	-40.4	8.6	-41.0	4.0	-16.2	-3.2	+3.2	-24.8	+7.0	-7.0	I
089.8-05.1	IC 5117	pn	11.44	1.17	732.8	-32.1	1.7	-21.0	2.0	-31.1	-2.1	+19.9	10.1	+23.7	-5.9	II
096.3+02.3	K3-61	[WC4-6]	11.49	1.07	207.6	-124.3	2.4	-109.0	2.0	-29.9	-3.3	+18.1	-79.1	+21.9	-7.1	III
096.4+29.9	NGC 6543	wels	8.27	0.08	801.1	-71.2	4.3	-65.0	2.0	-16.6	-2.1	+2.1	-48.4	+5.7	-5.7	II
100.6-05.4	IC 5217	wels	10.45	0.71	511.1	-114.3	2.4	-103.0	1.0	-37.7	-0.9	+5.7	-65.3	+9.5	-4.7	III
103.7+00.4	M 2-52	pn	10.56	0.71	36.7	-74.7	2.0	-70.0	2.0	-37.1	-1.8	+4.6	-32.9	+8.4	-5.6	I
104.4-01.6	M 2-53	pn	10.73	0.75	151.7	-81.8	1.9	-75.0	2.0	-35.7	-3.7	+3.9	-39.3	+7.7	-7.5	II
108.4-76.1	BoBn 1	pn	10.15	0.56	17007.0	190.9	3.0	198.0	2.0	2.3	-0.5	+1.4	195.7	+5.2	-4.3	halo
111.8-02.8	Hb 12	wels	18.74	2.61	696.1	-17.2	2.1	-8.0	1.0	404.0	-211.7	+293.9	-412.0	+297.7	-215.5	III

TABLE 4 (CONTINUED)

PN G	Name	Spectral type	R_G kpc	ΔR_G kpc	z pc	V_{hel}^a km s $^{-1}$	ΔV_{hel} km s $^{-1}$	V_{cat} km s $^{-1}$	ΔV_{cat} km s $^{-1}$	V_{circ} km s $^{-1}$	$\Delta V_{\text{circ}}(+)$ km s $^{-1}$	$\Delta V_{\text{circ}}(-)$ km s $^{-1}$	V_{pec} km s $^{-1}$	$\Delta V_{\text{pec}}(+)$ km s $^{-1}$	$\Delta V_{\text{pec}}(-)$ km s $^{-1}$	Peimbert Type
118.0-08.6	Vy 1-1	[WC]	12.85	1.17	1055.9	-47.4	5.1	-32.0	2.0	9.6	+36.0	-20.5	-41.6	+39.8	-24.3	II
118.8-74.7	NGC 246	PG1159	8.06	0.01	463.4	-69.1	0.3	-7.0	3.0	9.6	+0.1	-0.1	-16.6	+3.9	-3.9	II
119.6-06.7	Hu 1-1	pn	13.39	1.28	880.5	-67.5	3.1	-58.0	5.0	27.3	+47.7	-29.3	-85.3	+51.5	-33.1	III
120.0+09.8	NGC 40	[WC8]	8.58	0.12	182.1	-24.9	2.3	-25.0	3.0	-16.0	+3.0	-2.8	-9.0	+6.9	-6.6	II
130.2+01.3	IC 1747	[WO4]	10.22	0.48	68.7	-80.3	5.7	-79.0	2.0	-24.0	+3.6	-1.2	-55.0	+7.4	-5.0	II
130.3-11.7	M 1-1	pn	14.45	1.44	1641.4	-59.3	5.0	-34.0	1.0	65.3	+62.1	-42.1	-99.3	+65.9	-45.9	III
130.9-10.5	NGC 650-51	PG1159	8.99	0.21	261.7	-17.6	5.9	-22.0	3.0	-14.3	+3.7	-3.2	-7.7	+7.5	-7.0	II
133.1-08.6	M 1-2	pn	10.20	0.47	437.1	-28.3	5.5	-14.0	2.0	-20.5	+2.7	-1.2	6.5	+7.2	-5.0	II
144.5+06.5	NGC 1501	[WO4]	8.98	0.20	133.2	29.5	8.8	-8.5	-2.5	-2.5	38.0	+15.6	-15.4	II
146.7+07.6	M 4-18	[WC11]	16.17	1.71	1184.9	-64.2	18.8	-48.0	2.0	112.8	+76.3	-55.6	-160.8	+80.1	-59.4	III
159.0-15.1	IC 351	wels	13.27	1.07	1481.0	-31.1	2.0	-16.0	1.0	21.2	+14.9	-9.7	-37.2	+18.7	-13.5	III
161.2-14.8	IC 2003	[WC3]	12.42	0.90	1210.1	-22.7	4.7	-23.0	3.0	11.8	+7.8	-4.5	-34.8	+11.6	-8.3	II
166.1+10.4	IC 2149	pn	11.00	0.60	562.0	-38.2	5.2	-30.0	2.0	3.6	+0.0	0.0	-33.6	+4.9	-3.8	II
189.1+19.8	NGC 2371-72	[WO1]	9.75	0.35	634.8	22.0	1.0	19.0	+0.6	-0.7	3.0	+4.4	-4.5	II
194.2+02.5	J 900	wels	11.80	0.77	169.6	26.7	2.4	44.0	2.0	22.3	+1.7	-3.6	21.7	+5.5	-7.4	II
197.8+17.3	NGC 2392	pn	9.93	0.39	623.6	60.9	14.0	75.0	1.0	25.9	-1.4	-1.4	49.1	+4.7	-5.2	II
208.5+33.2	A 30	[WC]-PG1159	9.29	0.26	942.9	14.0	2.0	25.2	+1.8	-2.1	-11.2	+4.6	-6.0	II
243.3-01.0	NGC 2452	[WO1]	9.64	0.39	50.1	120.9	60.0	56.0	2.0	49.7	+3.9	-5.7	6.3	+7.5	-9.5	II
274.3+09.1	Lo 4	[WC]-PG1159	8.62	0.29	619.4
278.1-05.9	NGC 2867	[WO2]	8.00	0.06	231.7	14.4	1.1	18.9	+2.1	-2.0	-4.5	+15.0	-14.9	II
278.8+04.9	PB 6	[WO1]	8.54	0.34	381.9	56.0	1.0	30.9	+8.7	-10.1	25.1	+21.6	-30.0	I
285.4+01.5	Pe 1-1	[WO4]	8.90	0.66	172.0	34.7	0.3	36.3	+12.2	-17.6	-1.6	+25.1	-30.5	II
286.3+02.8	He 2-55	[WO3]	-27.3	3.5
291.3-26.2	Vo 1	[WC10]	-14.4	0.5
292.4+04.1	PB 8	[WN/WC]	8.56	0.74	527.9	15.5	1.0	27.3	+15.9	-22.4	-11.8	+28.8	-35.3	II
294.1+43.6	NGC 4361	pn	7.76	0.04	619.0	35.5	3.0	12.0	2.0	1.9	+1.1	-1.2	10.1	+5.0	-5.1	II
300.7-02.0	He 2-86	[WC4]	7.14	0.32	209.4	-6.7	0.2	-12.6	+12.2	-13.4	5.9	+25.1	-26.3	I
306.4-00.6	Th 2-A	[WO3]pec	6.82	0.16	26.18
307.2-03.4	NGC 5189	[WO1]	7.61	0.07	40.2	-15.6	0.5	-8.0	2.0	1.3	+2.4	-2.4	-16.9	+6.2	-6.2	I
307.5-04.9	MyCh 18	[WC]-PG1159	6.53	0.16	285.5	-68.0	2.0	-33.4	+6.6	-6.9	-34.6	+10.4	-10.7	I
309.0-04.2	He 2-99	[WC9]	6.34	0.15	279.3	-1.5	1.2	-40.4	+6.4	-6.6	38.9	+19.3	-19.5	II
309.1-04.3	NGC 5315	[WO4]	6.41	0.17	258.2
321.0+03.9	He 2-113	[WC10]	-60.4	0.8
322.4-00.1	Pe 2-8	[WR]/wels	5.05	0.26	8.8
327.1-02.2	He 2-142	[WC9]	4.41	0.26	287.4	-96.0	1.3	-96.8	+11.3	-11.8	0.8	+24.2	-24.4	II
332.9-09.9	He 2-133	[WC10]	-65.4	1.7
336.2-06.9	PC 14	[WC4]	3.45	0.43	738.5	-34.7	0.6	-103.9	+15.8	-16.7	69.2	+28.7	-29.6	III
337.4+01.6	Pe 1-7	[WC9]	3.71	0.59	148.4	-45.2	0.9	-92.4	+19.9	-21.7	47.2	+32.8	-34.6	II
355.2-02.5	H 1-29	[WC4]	3.56	0.88	155.0	-25.1	+6.4	-7.3	-2.6	+19.3	-20.2	bulge
355.9-04.2	M 1-30	wels	1.04	1.19	76.0	-119.0	0.4	-117.0	2.0	-40.4	+9.9	-11.3	-78.6	+13.7	-15.1	bulge
356.2-04.4	Ch 2-1	wels	0.54	0.28	622.0	-131.6	3.0	-169.0	3.0	-41.8	+2.5	-2.5	-127.2	+6.3	-6.3	bulge
358.3-21.6	IC 1297	[WO3]	3.39	0.92	1827.7	18.1	1.1	-8.9	+2.3	-2.6	27.0	+15.2	-15.5	II

Columns 1, 2, & 3: PNG#, common name and spectral types of central stars. Cols. 4, 5 & 6: galactocentric distance, error and height above the galactic plane.
^aCols. 7 & 8: heliocentric radial velocities from SPM or LCO (in boldface) and error. Cols. 9 & 10: heliocentric radial velocities and errors from SPM Kinematical catalogue. Cols. 11, 12, & 13: circular velocities from equation 1, and errors. Cols. 14, 15, & 16: peculiar velocities and errors. Col. 17: Peimbert's type.

TABLE 5
DISTRIBUTION OF OBJECTS ACCORDING
TO PEIMBERT TYPE

	Ty I	Ty II	Ty III	Bulge
[WR]PN ¹	10	23	5	5
WLPN	0	7	7	2
PN	2	6	3	–

¹[WR]PNe and [WR]-PG1159 included. The 9 missing [WR]PNe do not have known velocities or distances.

$V_{\text{pec}} = -89.6 \text{ km s}^{-1}$), PN G029.3–05.9 (NGC 6751, [WC]4, $V_{\text{pec}} = -62.5 \text{ km s}^{-1}$), PN G096.3+02.3 (K 3-61, [WC]4-5, $V_{\text{pec}} = -79.1 \text{ km s}^{-1}$), PN G146.7+07.6 (M 4-18, [WC]11, $V_{\text{pec}} = -160.8 \text{ km s}^{-1}$), and PN G336.2–06.9 (PC 14 [WO]4, $V_{\text{pec}} = -69.2 \text{ km s}^{-1}$). Finding Type III PNe among the [WR]PNe is peculiar because in § 2.1 we have shown that [WR]PNe are in general closer to the galactic plane than normal PNe and this would indicate that [WR]PNe are young objects. Among the few objects possessing z larger than 800 kpc (see Figure 1) only PN G146.7+07.6 (with $z = 1.19$ kpc) belongs to the Type III group.

One plausible explanation for these unexpected Type III [WR]PNe could be the errors in the adopted distances. For the objects with V_{pec} slightly above 60 km s^{-1} , the large V_{pec} error bars can move them into Type II's. However, there are at least three objects that would remain as genuine Type III: PN G002.4+5.8, PN G146.7+07.6, and PN G336.2–06.9. The first one, NGC 6369, is a well-known extended nearby PN. Stanghellini & Haywood (2010) attribute to it a heliocentric distance of 1.089 kpc, very similar to the distance given by Zhang (1995) of 0.92 kpc (with Zhang's distance we derive $V_{\text{pec}} = -89.1 \text{ km s}^{-1}$); therefore, the errors in the distance do not seem to be an explanation. Possibly the central star of NGC 6369 is an old low-mass star belonging to the thick disk, despite its [WR] condition and its small height above the galactic plane.

In the case of PN G146.7+07.6 (M 4-18) Stanghellini & Haywood (2010) locate it at a heliocentric distance of 8.96 kpc and at a galactocentric distance of 16.17 kpc; therefore, we derived a peculiar velocity of -160.8 km s^{-1} . If the heliocentric distance given by Zhang (1995) of 6.85 kpc is adopted, the galactocentric distance is 14.2 kpc, and the peculiar velocity turns out to be -91.5 km s^{-1} ; that is still large and would classify M 4-18 as a Type

III PN anyway. The distance given by Zhang (1995) is similar to the one derived independently by De Marco & Crowther (1999). In order to choose the more appropriate distance we can calculate the $H\beta$ luminosity of this object, by assuming the observed $\log(F(H\beta)) = -11.89$ (Acker et al. 1992) and the different heliocentric distances. When the distance by Stanghellini & Haywood (2010) is used, we get $\log(L(H\beta)/L_{\odot}) = 0.50$ which is slightly high for a PN (see Figure 5a by Peña, Stasińska, & Richer 2007), whereas using the distance by Zhang (1995) produces a $\log(L(H\beta)/L_{\odot}) = 0.27$, typical of a not too-bright PN. Thus, we consider that the distance by Zhang (1995) is more adequate for this [WR]PN, although it is still a Type III object and its central star would be a low mass object belonging to the thick disk.

For the case of PN G336.2–06.9 (PC 14), Stanghellini & Haywood (2010) heliocentric distance is 6.147 kpc, with a galactocentric distance of 3.451 kpc. This provides a $V_{\text{pec}} = 69.2 \text{ km s}^{-1}$. If the distance by Zhang (1995) of 5.11 kpc is used, V_{pec} turns out to be 51.3 km s^{-1} and the object would be a Type II.

Therefore in our [WR]PN sample, only NGC 6369 and M 4-18 would be *bona fide* Type III PNe.

Regarding non-[WR]PNe, we found three normal and seven WLPNe among Type III PNe which is an adequate number for normal objects and a little too high for WLPNe. As our numbers are small, in this case our results are only tentative.

4.4. The bulge objects

Apart from the two possibly bulge objects discussed in § 4.1, there are several PNe in our sample, for which we have determined heliocentric radial velocities, that have been classified as bulge PNe by some authors (Górny et al. 2009; Cavichia et al. 2011). As these objects do not rotate with the inner disk, it has not much sense to calculate their circular velocities. We have done it for completeness. Although the number of bulge objects in our sample is very small, it is interesting to analyze their heliocentric velocities in comparison with other samples of bulge PNe. We have PN G004.9+04.9 (M 1-25) with $V_{\text{hel}} = 10.3 \text{ km s}^{-1}$, PN G006.8+04.1 (M 3-15) with $V_{\text{hel}} = 96.9 \text{ km s}^{-1}$, PN G009.8–04.6 (H 1-67) with $V_{\text{hel}} = -15.0 \text{ km s}^{-1}$, PN G355.2–02.5 (H 1-29) with $V_{\text{hel}} = -27.7 \text{ km s}^{-1}$, PN G355.9–04.2 (M 1-30), with $V_{\text{hel}} = -117.0 \text{ km s}^{-1}$, and PN G356.2–04.4 (Cn 2-1) with $V_{\text{hel}} = -169.0 \text{ km s}^{-1}$. The heliocentric velocities of these objects are mainly positive when the galactic longitude l is between 0° and 10° , and negative when l is between 0° to -10° . In this

sense, they behave similarly to the sample discussed by Durand et al. (1998, see their Figure 6), who have interpreted this behavior as rotation of the bulge.

4.5. *Special cases*

Among our PNe there are two objects with a very large V_{pec} . One is PN G108.4-76.1 (BoBn 1), a very interesting PN with a strange chemical composition as it shows Ne/O larger than 1 (Peña et al. 1993; Otsuka et al. 2010), identified it as belonging to the galactic halo at a very large height above the plane (17 kpc). Zijlstra et al. (2006) have argued that this object could be part of the Sagittarius Dwarf Spheroidal galaxy, which is supported by the PN galactic position and its large V_{pec} (195.7 km s^{-1}).

Another PN with extremely high V_{pec} (-412.0 km s^{-1}) is PN G111.8-02.8 (Hb 12) but this could be due to a possibly erroneous heliocentric distance of 14.25 kpc (galactocentric distance 18.47 kpc) given by Stanghellini & Haywood (2010). The heliocentric distance of 8.11 kpc, given by Zhang (1995), locates the object much closer and its galactocentric distance becomes 13.34 kpc. With this, we derive a much more reasonable V_{pec} of -32.9 km s^{-1} . In addition, if we calculate the total $H\beta$ luminosity for this object (taking the apparent $H\beta$ flux by Acker et al. 1992, $\log(F(H\beta))=10.98$), for a distance of 14.25 kpc, we get $\log(L(H\beta)/L_{\odot})=1.82$, which is too high for a PN and more typical of a compact HII region (see again Figure 5a by Peña et al. 2007). When assuming the distance by Zhang (1995), we obtain $\log(L(H\beta)/L_{\odot})=1.33$, which is an adequate $H\beta$ luminosity for a bright PN. Therefore we consider than the distance by Stanghellini & Haywood (2010) might be erroneous.

5. CONCLUSIONS

From high-quality high spectral resolution spectra we have determined the heliocentric radial velocities for a sample of [WR]PNe (44 objects, representing the 42% of the total known sample), a sample of WLPNe and PNe with normal central star. These data, together with distances obtained from the literature, allowed us to determine the galactic kinematics of the objects. The radial circular and peculiar velocities were computed. We found that these quantities are largely affected by errors in the assumed distances and for some objects where too large V_{pec} are obtained, this can be attributed to poorly determined distances.

We have found that most of the analyzed [WR]PNe are located in the galactic disk and they

are more concentrated towards the thin disk (height smaller than about 400 pc from the disk) than the WLPNe and PNe with normal central star, most of which are distributed up to 800 pc from the disk.

According to their chemical composition and peculiar velocities we have classified the studied sample in Peimbert's Types. Nine [WR]PNe (21%) and one [WR]-PG1159 PN have been classified as Peimbert's Type I (they are N- and He-rich) and would have progenitor stars with initial masses larger than $2 M_{\odot}$. Therefore, they would be young objects (ages between 0.1 to 1 Gyr). This is confirmed by their kinematics as all of them (except two objects of the bulge) show V_{pec} smaller than 50 km s^{-1} .

The [WR]PNe with $V_{\text{pec}} \leq 60 \text{ km s}^{-1}$ and no particular He or N enrichment, amounting to 23 objects (51% of the sample), are catalogued as Peimbert's Type II. They belong to the disk population and would be of intermediate age. Interestingly, there are a five [WR]PNe with V_{pec} larger than 60 km s^{-1} which are classified as Type III PNe. Although some of them could be of Type II by considering the uncertainties in their distances, there are two objects which appear as genuine Type III [WR]PNe. With this classification, these objects would belong to the thick disk with an old low-mass central star, indicating that the [WR] phenomenon can occur also in less massive and old progenitors.

In our sample of 16 WLPNe, none is a Peimbert Type I, a result also found by other authors in the analysis of larger samples (e.g., Fogel et al. 2003). Our WLPNe are distributed in 7 of Type II, 7 of Type III and 2 bulge objects. With these characteristics WLPNe are objects belonging to the intermediate and old disk population, with progenitors of low initial masses. Thus, it is corroborated that [WR]PNe and WLPNe are unrelated objects.

We have obtained the radial velocity of the [WR] PN G332.9-09.9 (He3-1333 whose central star, CPD-56 8032, has a [WC]10 spectral type) that has not been reported previously. Its heliocentric distance is not reported in the literature, therefore its peculiar velocity cannot be calculated.

J.S.R.-G. acknowledges scholarship from Conacyt-Mexico. J.G.-R. received financial support from the spanish Ministerio de Educación y Ciencia (MEC), under project AYA2007-63030. This work received financial support from DGAPA-Universidad Nacional Autónoma de México (PAPIIT project IN105511).

REFERENCES

- Allen, C., Carigi, L., & Peimbert, M. 1998, *ApJ*, 494, 247
- Acker, A., Górny, S. K., & Cuisinier, F. 1996, *A&A*, 305, 944
- Acker, A., Marcout, J., Ochsenbein, F., Stenholm, B., Tylenda, R., & Schohn, C. 1992, *Strasbourg-ESO Catalogue of Galactic Planetary Nebulae* (Garching: ESO)
- Acker, A., & Neiner, C. 2003, *A&A*, 403, 659
- Akras, S., & López, J. A. 2012, *MNRAS*, 425, 2197
- Bernstein, R. A., Shectman, S. A., Gunnels, S., Mochnicki, S., & Athey, A. 2003, *Proc. SPIE*, 4841, 1694
- Cavichia, O., Costa, R. D. D., & Maciel, W. J. 2011, *RevMexAA*, 47, 49
- De Marco, O., & Crowther, P. A. 1999, *MNRAS*, 306, 931
- DePew, K., et al. 2011, *MNRAS*, 414, 2812
- Durand, S., Acker, A., & Zijlstra, A. A. 1998, *A&AS*, 132, 13
- Fogel, J., De Marco, O., & Jacoby, G. 2003, in *IAU Symp. 209, Planetary Nebulae: Their Evolution and Role in the Universe*, ed. S. Kwok, M. Dopita, & R. Sutherland (San Francisco: ASP), 235
- García-Rojas, J., Peña, M., Morisset, C., Mesa-Delgado, A., & Ruiz, M. T. 2012, *A&A*, 538, 54
- García-Rojas, J., Peña, M., & Peimbert, A. 2009, *A&A*, 496, 139
- Gesicki, K., Zijlstra, A. A., Acker, A., Górny, S. K., Goździewski, K., & Walsh, J. R. 2006, *A&A*, 451, 925
- Górny, S. K., Chiappini, C., Stasińska, G., & Cuisinier, F. 2009, *A&A*, 500, 1089
- Górny, S. K., & Stasińska, G. 1995, *A&A*, 303, 893
- Howard, J. W., Henry, R. B. C., & McCartney, S. 1997, *MNRAS*, 284, 465
- Kerr, F. J., & Lynden-Bell, D. 1986, *MNRAS*, 221, 1023
- Kingsburgh, R. L., & Barlow, M. J. 1994, *MNRAS*, 271, 257
- Koesterke, L. 2001, *Ap&SS*, 275, 41
- Levine, S., & Chakrabarty, D. 1994, *Reporte Técnico MU-94-04* (Mexico: IA-UNAM)
- López, J. A., et al. 2012, *RevMexAA*, 48, 3
- Medina, S., Peña, M., Morisset, C., & Stasinska, G. 2006, *RevMexAA*, 42, 53
- Mihalas, D., & Roustly, P. M. R. 1968, *Galactic Astronomy*, ed. G. Burbidge & M. Burbidge (San Francisco: W. H. Freeman), 101
- Otsuka, M., Tajitsu, A., Hyung, S., & Izumiura, H. 2010, *ApJ*, 723, 658
- Peimbert, M. 1978, in *IAU Symp. 76, Planetary Nebulae*, ed. Y. Terzian (Dordrecht: Reidel), 215
- Peimbert, M. 1990, *Rep. Prog. Phys.*, 53, 1559
- Peimbert, M., Luridiana, V., & Torres-Peimbert, S. 1995, *RevMexAA*, 31, 147
- Peimbert, M., & Serrano, A. 1980, *RevMexAA*, 5, 9
- Peimbert, M., & Torres-Peimbert, S. 1983, in *IAU Symp. 103, Planetary Nebulae* ed. D. R. Flower (Dordrecht: Reidel), 233
- Peña, M., & Medina, S. 2002, *RevMexAA*, 38, 23
- Peña, M., Medina, S., & Stasinska, G. 2003, *RevMexAA (SC)*, 18, 84
- Peña, M., Stasińska, G., & Medina, S. 2001, *A&A*, 367, 983
- Peña, M., Stasińska, G., & Richer, M. G. 2007, *A&A*, 476, 745
- Peña, M., Torres-Peimbert, S., Peimbert, M., & Dufour, R. J. 1993, *RevMexAA*, 27, 175
- Reid, M. T. 1993, *ARA&A*, 31, 345
- Stanghellini, L., & Haywood, M. 2010, *ApJ*, 714, 1096
- Stasińska, G., & Tylenda, R. 1994, *A&A*, 289, 225
- Todt, H., Peña, M., Hamann, W.-R., & Gräfener, G. 2010, *A&A*, 515, 83
- Weidmann, W. A., & Gamen, R. 2011, *A&A*, 526, A6
- Zhang, C. Y. 1995, *ApJS*, 98, 659
- Zijlstra, A. A., Gesicki, K., Walsh, J. R., Péquignot, D., Van Hoof, P. A. M., & Minniti, D. 2006, *MNRAS*, 369, 875

M. Peña and J. S. Rechy-García: Instituto de Astronomía, Universidad Nacional Autónoma de México. Apdo. Postal 70-264, México D.F., 04510, Mexico (miriam, jrechy@astro.unam.mx).

J. García-Rojas: Instituto de Astrofísica de Canarias, Vía Láctea s/n, E-38200, La Laguna, Tenerife, and Departamento de Astrofísica, Universidad de la Laguna, E-38205, La Laguna, Tenerife, Spain (jogarcia@iac.es).